INDEX COPERNICUS INTERNATIONAL

Bio-Algorithms and Med-Systems

WWW.BAMSJOURNAL.COM ISSN: 1896-530X

ORIGINAL ARTICLE

Received: 27.11.2023
Accepted: 22.12.2023
Published: 31.12.2023

CITE THIS ARTICLE AS:
Mryka W, Manish Das M, Beyene EY, Moskal P, Stępien E, On behalf of J-PET collaboration, "Estimating influence of positron range in proton-therapy-beam monitoring with PET," Bio--Algorithms and Med--Systems vol. 1, no. 1, pp. 96-100, 2023, DOI: 10.5604/01.3001.0054.1939

CORRESPONDING AUTHOR:
Wiktor Mryka; Department of Experimental Particle Physics and Applications, Faculty of Physics, Astronomy and Applied Computer Science, Jagiellonian University, Krakow, Poland; Łojasiewicza street 11, 30-348 Kraków, Poland; E-mail: w.mryka@doctoral.uj.edu.pl

Estimating influence of positron range in proton-therapy-beam monitoring with PET

Wiktor Mryka[1,2] (ORCID: 0009-0006-7616-8290), Manish Das[1,2] (ORCID: 0009-0001-2901-1745), Ermias Y. Beyene[1,2] (ORCID: 0009-0002-8757--2169), Paweł Moskal[1,2] (ORCID: 0000-0002-4229-3548), Ewa Stępień[1,2] (ORCID: 0000-0003-3589-1715), On behalf of J-PET collaboration

[1]Faculty of Physics, Astronomy and Applied Computer Science, Jagiellonian University, Krakow, Poland
[2]Centre for Theranostics, Jagiellonian University, Krakow, Poland

ABSTRACT

The application of PET scanners to proton-beam-therapy monitoring is a promising solution to obtain the range of the beam and hence the positions of a Bragg peak – maximum dose deposition point. A proton beam induces nuclear reactions in the tissue, leading to the production of isotopes that emit β^+ radiation. This enables the imaging of the density distribution of β^+ isotopes produced in the body, allowing the reconstruction of the proton beam range. Moreover, PET detectors may open the possibility for in-beam monitoring, which would offer an opportunity to verify the range during irradiation. PET detectors may also allow positronium imaging, which would be the indicator of the tissue conditions. However, the image of annihilation points does not represent the range of the proton beam. There are several factors influencing the translation from annihilation points to obtain the Bragg peak position. One of them is the kinetic energy of the positron. This energy corresponds to some range of the positron within the tissue. In this manuscript we estimate positron energy and its range and discuss its influence on proton therapy monitoring.

KEYWORDS

proton therapy, positron range, positron emission tomography (PET), beta spectra, proton beam monitoring

LIST OF ABBREVIATIONS

PET – positron emission tomography
CT – computed tomography
HU – Hounsfield units
SPV – stopping power units
H-L – half-life/half-lives

INTRODUCTION

Proton therapy is a quickly developing type of radiotherapy [1–5]. Using its advantages – finite range of protons, maximum energy deposition at the end of the path (Bragg peak) and steep gradient of the dose – one can obtain more uniform dose distribution and better coverage of a tumor volume than in/with conventional radiotherapy techniques. At the same time, low-energy deposition in the early stage of its path reduces the dose in healthy tissues surrounding the tumor. To fully exploit these advantages one needs to precisely know the position of a Bragg peak in the tissue [6–8]. Standard techniques rely on the images of patients (computed tomography, CT).

Later, dedicated programs based on Monte Carlo simulations performed computations to extract information of stopping power values from CT images and their relation to stopping the power of water. This required conversion of the Hounsfield units (HU) into stopping power values (SPV). Utilizing the experimentally obtained Bragg peak position in water, programs computed the Bragg peak position in a patient's tissue. This approach depended on many factors, such as a patient's anatomy, positioning during imaging and the quality of HU-SPV conversion.

So far, the therapy relies on pretreatment planning and simulations, which influences the treated volume – one needs to take some margins to make certain that the tumor volume is covered by the planned dose. Having the beam endpoint in the patient's body would result in shrinking those margins to bare minimum, limited only to the resolution of the monitoring system, and obtaining more conformal dose distribution in the treated volume. Moreover, obtaining a precise beam-range monitoring system would be crucial in FLASH proton therapy, which aims to deliver a huge dose (compared to current standards) with one irradiation process [9, 10]. To enable the verification of the proton beam range in a patient's body it is proposed to use a PET detector. This will enhance the therapy process as the posttreatment verification and, possibly, the in-beam monitoring may lead to more precise irradiation of the tumor volume.

The PET detector registers annihilation quanta coming from positron-electron annihilation caused by β^+ radiation from the radioisotopes distributed to the patient. Protons interact with matter due to electromagnetic interactions, scattering on nuclei or nuclear reactions. The latter, although they account for only a fraction of all interactions, are crucial for beam range monitoring. A fraction of nuclear reactions caused by protons produce radioisotopes – β^+ emitters. Some of those radioisotopes have a short lifetime and thus can enable in-beam monitoring. Long--lived ones can serve for verification of the range off-beam [11, 12]. However, what one can reconstruct from the signal registered are the annihilation points, but needed are the nuclear reaction positions. To obtain them one needs to make a chain of corrections. The aim of this study is to estimate the maximum and mean range of positrons emitted from radioisotopes induced by a proton beam.

PROTON THERAPY MONITORING

Multi-isotope imaging could be an applicable implement in proton therapy monitoring. Our focus is devoted to β^+ isotopes, as those are necessary for PET beam-range monitoring and positronium imaging. The main reaction channels are listed in Tab. I., together with primary atoms and produced β^+ isotopes.

Tab. I. Table of nuclear reactions induced by the proton beam with different targets, reaction channels and produced β^+ emitters.

PRIMARY ATOM	NUCLEAR REACTION	β^+ ISOTOPE
C	$^{12}C(p,pn)^{11}C$	^{11}C
	$^{12}C(p,p2n)^{10}C$	^{10}C
N	$^{14}N(p,2p2n)^{11}C$	^{11}C
	$^{14}N(p,pn)^{13}N$	^{13}N
	$^{14}N(p,n)^{14}O$	^{14}O
O	$^{16}O(p,pn)^{15}O$	^{15}O
	$^{16}O(p,3p3n)^{11}C$	^{11}C
	$^{16}O(p,2p2n)^{13}N$	^{13}N
	$^{16}O(p,p2n)^{14}O$	^{14}O
	$^{16}O(p,3p4n)^{10}C$	^{10}C
P	$^{31}P(p,pn)^{30}P$	^{30}P
Ca	$^{40}Ca(p,2pn)^{38}K$	^{38}K

One can distinguish two stages of range monitoring: in-beam and off-beam. The first stage takes place during irradiation and can be a primary indicator of any necessary corrections. In Tab. I. one can see that two isotopes are suitable for in-beam monitoring, considering their short H-L – ^{10}C and ^{14}O. They are also important for another reason. Both ^{10}C and ^{14}O, after emitting positron, also emit prompt gamma, on average after 710 ps and 68 fs, respectively, with an energy of 0.718 MeV in case of ^{10}C, and 2.313 MeV in case of ^{14}O [13]. Simultaneous measurement of annihilation photons and prompt gamma enables the imaging of positronium properties in the tissue using the positronium imaging method [14–17]. Positronium is considered as a biomarker of hypoxia [18, 19]. Off-beam range monitoring can use signal (annihilation

gammas) from remaining longer-lived isotopes to confirm range verification with better precision.

It needs to be noted that the reconstructed gamma annihilation points will not be sufficient to determine the actual, total proton beam range [6, 20]. This is due to two major factors – protons at the end of their path have insufficient energy to produce isotopes, and emitted positrons have kinetic energy, which corresponds to some range in the tissue. In this paper the second element is taken into consideration.

METHODS

Beta spectra

The energy of the positron in β^+ decay vary from 0 to some maximum energy E_{max}, which is different for each isotope. The probable density distribution of energy of the emitted positron (energy spectrum) dn/dE_{e+} can be described using the following formula [21, 22]:

$$\frac{dn}{dE_{e^+}} = A\sqrt{E_{e^+}^2 + 2E_{e^+}m_e}\cdot(E_{max} - E_{e^+})^2\cdot(E_{e^+} + m_e) \quad (1)$$

where A is a normalization factor, E_{max} is maximum energy of emitted positron, and m_e the mass of a positron [23, 24]. The normalization factor A is chosen so that the area under the curve is equal to unity.

Positron range

Since an emitted positron carries kinetic energy, it will be moving from the point of emission. Thus, knowing its kinetic energy one can determine its range. We follow Cal-Gonzalez et al., who use the semiempirical model, proposed by Katz and Penfold, to give analytical formulas for determining maximum and mean positron range in water [25, 26]. The formula for the mean positron range yields:

$$R_{mean} \approx \frac{0.108(E_{e^+}(MeV))^{1.14}}{\rho(g\cdot cm^{-3})} \quad (2)$$

where ϱ is the density of the medium and E_{e+} is the positron energy. For calculating the maximum range the formulas are:

$$R_{max} \approx \frac{412\left(E_{e^+}(MeV)\right)^n}{\rho(mg\cdot cm^{-3})}; 0.01 \le E_{e^+} \le 2.5MeV \quad (3)$$

$$R_{max} \approx \frac{530E_{e^+}(MeV) - 106}{\rho(mg\cdot cm^{-3})}; 2.5 \le E_{e^+} \le 20MeV \quad (4)$$

where $n = 1.265 - 0.0954\cdot ln(E_{e+}(MeV))$.

RESULTS

Beta spectra

The beta spectra for isotopes listed in Tab. I. are shown in Fig. 1. and 2.

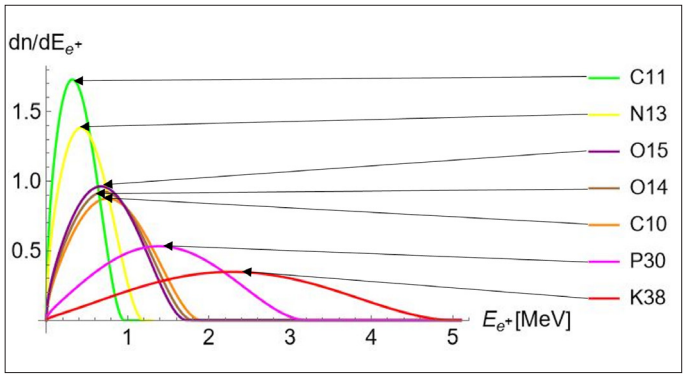

Fig. 1. Beta spectra for the isotopes produced during irradiation with a proton beam. All are normalized to unity.

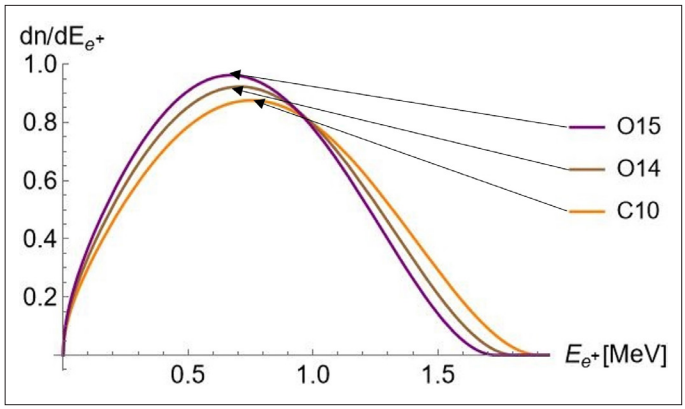

Fig. 2. Shows only the overlapping spectra of ^{14}O, ^{15}O and ^{10}C Positron range.

In Tab. II. we listed isotopes, their half-lives (H-L), the maximum and mean energy of emitted positrons and the corresponding range of the positron. In Fig. 3. and 4. we present a graphical representation of positron ranges.

DISCUSSION

The results shown in Fig. 3. and 4. indicate that the positrons emitted by β^+ isotopes produced by a proton beam in the tissue will smear the PET image at the order of 2 mm and need to be taken into account when developing PET-based proton-beam--range monitoring with precision better than 1 mm.

We also calculated the mean positron range for two other β^+ emitters and compared the results with the work of [27]. The

Tab. II. Shows the list of isotopes induced in reactions with the proton beam shown in Tab. I. together with their half-lives (H-L) and maximum and mean energy of emitted positrons. With each energy the table shows the maximum and mean range of the positron calculated with eqs 2, 3 and 4.

β^+ ISOTOPE	H-L	E_{MAX} [keV]	R_{MAX} [mm]	R_{MEAN} [mm]	E_{MEAN} [keV]	R_{MAX} [mm]	R_{MEAN} [mm]
^{10}C	19.29 s	1908	9.0	2.3	814	3.2	0.9
^{11}C	20.33 min	960	3.9	1.0	386	1.1	0.4
^{13}N	9.96 min	1199	5.2	1.3	492	1.6	0.5
^{14}O	70.61 s	1808	8.5	2.1	771	3.0	0.8
^{15}O	122.24 s	1732	8.0	2.0	735	2.8	0.8
^{30}P	2.50 min	3210	16.0	4.1	1441	6.4	1.6
^{38}K	7.64 min	5022	25.6	6.8	2323	11.2	2.8

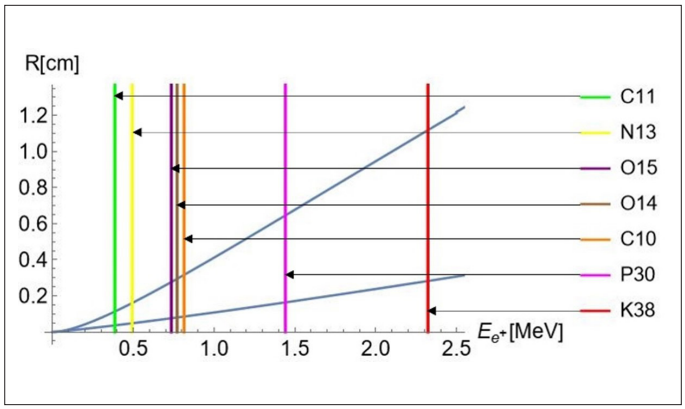

Fig. 3. Plot showing maximum and mean positron range as a function of positron energy, calculated using eq. 2, eq. 3 and eq. 4 (blue lines). Vertical lines show mean values of positron energies for different isotopes.

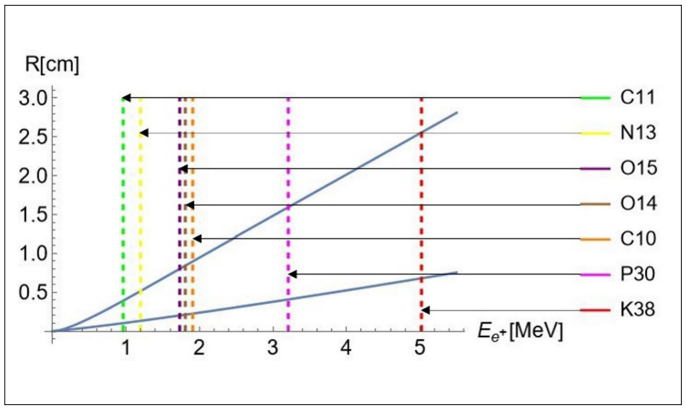

Fig. 4. Plot showing maximum and mean positron range as a function of positron energy, calculated using eq. 2, eq. 3 and eq. 4 (blue lines). Vertical, dashed lines show maximum values of positron energies for different isotopes.

results are shown in Tab. III. The comparison show that the results obtained in this work for those isotopes are in an agreement with [27] within 3%.

Tab. III. Table of mean range of positrons for chosen isotopes compared between this work and [27].

		THIS WORK	REF. [27]
β^+ ISOTOPE	E [keV]	R_{MEAN} [mm]	R_{MEAN} [mm]
^{68}Ga	1899	2.25	2.32
^{124}I	1822	2.15	2.28

CONCLUSIONS

The results presented here are the first step to prepare the correction chain needed to properly translate data, i.e., annihilation points to the Bragg peak point. Differences observed in positron energies and the mean and maximum range of positrons in the tissue shows that considering the positron range it may be more complex. If one wants to apply in-beam monitoring it needs to be considered that many isotopes will be produced at once and positrons from different β^+ emitters will contribute to the PET image. Therefore, for the estimations of the effect of the positron range on PET images in proton-beam-range monitoring it will be necessary to take into account the convolution of the production cross section of different isotopes with the positrons' energy spectra, and the dependence of the positron range on its energy. This contribution constitutes a preparatory step for this research.

ACKNOWLEDGEMENTS

We acknowledge support from the Foundation for Polish Science through the TEAM POIR.04.04.00-00-4204/17 program, the National Science Centre of Poland through grant nos. 2021/42/A/ST2/00423 and 2021/43/B/ST2/02150, Jagiellonian University via Project No. CRP/0641.221.2020 and the SciMat and qLife Priority Research Area budget under the auspices of Excellence Initiative – Research University at Jagiellonian University.

REFERENCES

1. Parodi K, Yamaya T, Moskal P. Experience and new prospects of PET imaging for ion beam therapy monitoring. Z. Med. Phys. 2023;33:22-34.
2. Durante M, Loeffler J. Charged particles in radiation oncology. Nat Rev Clin Oncol 2010;7:37-43.
3. Graeff C, Volz L, Durante M. Emerging technologies for cancer therapy using accelerated particles. Prog. Part. Nucl. Phys. 2023;131:104046.
4. Durante M, Orecchia R, Loeffler JS. Chargedparticle therapy in cancer: clinical uses and future perspectives. Nat Rev Clin Oncol. 2017;14(8):483-95.
5. Nystrom H, Jensen MF, Nystrom PW. Treatment planning for proton therapy: what is needed in the next 10 years? Br J Radiol. 2020;93(1107):20190304.
6. Brzeziński K, Baran J, Borys D, Gajewski J, Chug N, Coussat A, et al. Detection of range shifts in proton beam therapy using the J-PET scanner: a patient simulation study. Phys. Med. Biol. 2023;68:145016.
7. Jäkel O. Physical advantages of particles: protons and light ions. Br J Radiol 2020;93:20190428.
8. Lang K. Towards high sensitivity and highresolution PET scanners: imaging-guided proton therapy and total body imaging. Bio-Algorithms and Med-Systems 2022;18:96-106.
9. Abouzahr F, Cesar JP, Crespo P, Gajda M, Hu Z, Kaye W, et al. The first PET glimpse of a proton FLASH beam. Phys. Med. Biol. 2023;68:125001.
10. Abouzahr F, Cesar JP, Crespo P, Gajda M, Hu Z, Klein K, et al. The first probe of a FLASH proton beam by PET Phys. Med. Biol. 2023;68:235004.
11. Purushothaman S, Kostyleva D, Dendooven P, Haettner E, Geissel H, Schuy C, et al. Quasi-real-time range monitoring by in-beam PET: a case for 15O. Sci Rep 2023;13:18788.
12. Rucinski A, Baran J, Garbacz M, Pawlik-Niedzwiecka M, Moskal P. Plastic scintillator based PET detector technique for proton therapy range monitoring: A Monte Carlo study. 2018 IEEE Nuclear Science Symposium and Medical Imaging Conference, NSS/MIC 2018 - Proceedings' pp. 24-7.
13. Das M, Mryka W, Beyene EY, Parzych S, Sharma S, Stępień E, et al. Estimating the efficiency and purity for detecting annihilation and prompt photons for positronium imaging with J-PET using toy Monte Carlo simulations. Bio-Algorithms and Med-Systems 2023;19:87-95.
14. Moskal P. Positronium imaging. In: 2019 IEEE Nuclear Science Symposium and Medical Imaging Conference (NSS/MIC). Manchester, UK: IEEE Xplore; 2020.
15. Moskal P, Kisielewska D, Curceanu C, Czerwiński E, Dulski K, Gajos A, et al. Feasibility study of the positronium imaging with the J-PET tomograph. Phys Med Biol 2019;64:055017.
16. Moskal P, Dulski K, Chug N, Curceanu C, Czerwiński E, Dadgar M, et al. Positronium imaging with the novel multiphoton PET scanner. Sci Adv 2021;7:eabh4394.
17. Bass SD, Mariazzi S, Moskal P, Stępień E. Colloquium: Positronium physics and biomedical applications. Rev. Mod. Phys. 2023;95:021002.
18. Moskal P, Stępień EŁ. Positronium as a biomarker of hypoxia. Bio-Algorithms and Med-Systems 2021;17(4):311-9.
19. Shibuya K, Saito H, Nishikido F, Takahashi M, Yamaya T. Oxygen sensing ability of positronium atom for tumor hypoxia imaging. Commun Phys 2020;3:173.
20. Paganetti H. Range uncertainties in proton therapy and the role of Monte Carlo simulations. Phys Med Biol 2012;57:R99.
21. Blatt J, Weisskopf V. Theoretical nuclear physics. Verlag: Springer; 2012.
22. Evans RD. The Atomic Nucleus. Montgomery, USA: Krieger Pub Co; 1982.
23. https://wwwnds.iaea.org [Internet]. IAEA. International atomic energy agency, live chart of nuclides [cited: 2023 Dec 03]. Available from: https://wwwnds.iaea.org/relnsd/vcharthtml/VChartHTML.html.
24. http://www.nist.gov [Internet]. National Institute of Standards and Technology [cited: 2023 Sept 30]. Available from: http://www.nist.gov/.
25. Cal-González J, Herraiz JL, España S, Corzo PMG, Vaquero JJ, Desco M, et al. Positron range estimations with PeneloPET. Phys. Med. Biol. 2013;58:5127.
26. Katz L, Penfold AS. Rev. Mod. Phys. 1952;24:28-44.
27. Kertész H, Beyer T, Panin V, Jentzen W, Cal-Gonzalez J, Berger A, et al. Implementation of a Spatially-Variant and Tissue-Dependent Positron Range Correction for PET/CT Imaging. Front. Physiol. 2022;13:818463.